

RESEARCH ARTICLE

Multimodal *in vivo* staging in amyotrophic lateral sclerosis using artificial intelligence

Anna Behler¹, Hans-Peter Müller¹, Kelly Del Tredici¹, Heiko Braak¹, Albert C. Ludolph^{1,2},
Dorothee Lulé¹ & Jan Kassubek^{1,2} 

¹Department of Neurology, University of Ulm, Germany

²Deutsches Zentrum für Neurodegenerative Erkrankungen (DZNE), Ulm, Germany

Correspondence

Jan Kassubek, Department of Neurology,
University of Ulm, Oberer Eselsberg 45,
89081 Ulm, Germany. Tel: + 49 731
1771206; Fax: + 49 731 1771202; E-mail:
jan.kassubek@uni-ulm.de

Funding Information

This study was supported by the German
Research Foundation (Deutsche
Forschungsgemeinschaft, DFG Grant Number
LU 336/15-1) and the German Network for
Motor Neuron Diseases (BMBF 01GM1103A).

Received: 14 March 2022; Revised: 10 May
2022; Accepted: 26 May 2022

*Annals of Clinical and Translational
Neurology* 2022; 9(7): 1069–1079

doi: 10.1002/acn3.51601

Abstract

Background: The underlying neuropathological process of amyotrophic lateral sclerosis (ALS) can be classified in a four-stage sequential pTDP-43 cerebral propagation scheme. Using diffusion tensor imaging (DTI), *in vivo* imaging of these stages has already been shown to be feasible for the specific corticofugal tract systems. Because both cognitive and oculomotor dysfunctions are associated with microstructural changes at the brain level in ALS, a cognitive and an oculomotor staging classification were developed, respectively. The association of these different *in vivo* staging schemes has not been attempted to date. **Methods:** A total of 245 patients with ALS underwent DTI, video-oculography, and cognitive testing using Edinburgh Cognitive and Behavioral ALS Screen (ECAS). A set of tract-related diffusion metrics, cognitive, and oculomotor parameters was selected for further analysis. Hierarchical and *k*-means clustering algorithms were used to obtain an optimal cluster solution. **Results:** According to cluster analysis, differentiation of patients with ALS into four clusters resulted: Cluster A showed the highest fractional anisotropy (FA) values and thereby the best performances in executive oculomotor tasks and cognitive tests, whereas cluster D showed the lowest FA values, the lowest ECAS scores, and the worst executive oculomotor performance across all clusters. Clusters B and C showed intermediate results regarding parameter values. **Discussion:** In a multimodal dataset of technical assessments of brain structure and function in ALS, an artificial intelligence-based cluster analysis showed high congruence of DTI, executive oculomotor function, and neuropsychological performance for mapping *in vivo* correlates of neuropathological spreading.

Introduction

Amyotrophic lateral sclerosis (ALS) is characterized by the progressive degeneration of both upper motor neurons and lower motor neurons, which is fatal after an average of 3 years.¹ Despite the clinical emphasis on motor deficits, ALS is now regarded a multisystem disorder.² At motor onset, depending on cutoffs for neuropsychological tests – up to 50% of patients show cognitive impairment and/or behavioral changes^{3,4}; although evidence for worsening in advanced disease is equivocal.^{5–8} Although not a predominant symptom, a number of mostly subclinical oculomotor alterations has been observed in patients with ALS.^{9,10}

Anatomical post-mortem analyses show that the distribution of phosphorylated 43 kDa TAR DNA-binding protein (pTDP-43) follows a sequential pattern with four neuropathological stages in the central nervous system.^{11,12} Initially, the ALS pathology spreads from the motor neocortex via corticofugal pathways toward the spinal cord and brainstem,¹³ then to the frontal, parietal and, finally, anteromedial temporal lobes.¹⁴ Diffusion tensor imaging (DTI) has been used for the *in vivo* analysis of white matter neuronal pathways and, thus, the identification of pathways associated with sequential ALS progression.¹⁵ A characterization of the microstructural properties of the involved tract systems based on fractional anisotropy (FA) allowed for an *in vivo* staging

classification at individual level and quantitative mapping of disease progression in the brain.¹⁶

Inasmuch as regional microstructural changes and different cognitive domains are closely linked, cognitive symptoms show a distinct pattern for *in vivo* staging of cognition.³ In cognitively impaired patients with ALS, altered executive functions showed congruence with DTI-based stage 2, disinhibited behavior with stage 3, and impaired memory with stage 4. Eye movement dysfunctions measured with video-oculography (VOG) are also associated with brain dysfunction in ALS and have been characterized by a sequential pattern parallel to the first two neuropathological stages.¹⁷ Thereby, VOG stage 1 is confined to executive oculomotor deficits, that is, increased anti-saccade error rates, saccadic intrusions, or a lower number of voluntary gaze shifts, whereas VOG stage 2 is associated with prolonged reactive saccades and disturbed smooth pursuit eye movements. Although the type of affected oculomotor parameters suggests conclusions to be drawn about the brain regions involved, there is still a missing link between the alignment of the VOG staging pattern with the DTI pattern, on the one hand, and the cognitive staging pattern on the other.

Here, we provide an approach to differentiate groups of patients with ALS according to DTI, cognitive, and oculomotor parameters using artificial intelligence (AI), that is, unsupervised clustering algorithms which are able to explore complex datasets.¹⁸ In multivariate datasets, these methods can identify groups of data with similar measurement results without prior knowledge of class membership.

Given the advantages of AI over traditional patient classification strategies,¹⁹ the current study aims to show whether the microstructural, oculomotor, and cognitive alterations in patients with ALS are associated with one another and whether the joint analysis of the three domains can serve as a marker for the stratification of the neuropathological disease stage.^{11,12} Multimodal approaches are prospective advances for patient classification early in the disease course to facilitate timely inclusion in individualized therapeutic trials in the future. Thus, an AI clustering approach is introduced as a novel multimodal technique to improve the results of previously established techniques.^{3,15,17}

Materials and Methods

Participants

For this study, we collected data from 245 patients (146 male/99 female) with clinically definite or probable sporadic ALS according to the revised El Escorial diagnostic criteria²⁰ who received a magnetic resonance imaging

(MRI)-based DTI scan, a VOG examination, and neuropsychological testing within 2 weeks between the years 2013 and 2021. None of the patients had any clinically suspected form of dementia and/or clinical signs of frontotemporal lobar degeneration. Severity of physical symptoms was measured with the revised ALS functional rating scale (ALS-FRS-R).²¹ Detailed sample characteristics are given in Table 1. In addition, VOG data of 64 healthy controls (age 50.6 ± 13.4 years, 37 male/27 female) and MRI data of 75 healthy controls (age 60.0 ± 13.4 years, 39 male/36 female) were used. Those two groups of healthy controls were completely independent.

All participants provided written consent according to institutional guidelines, and the study was approved by the Ethics Committee of the University of Ulm, Germany (reference # 19/12).

MRI data acquisition and processing

DTI datasets were acquired on a 1.5 T clinical scanner (Magnetom Symphony, Siemens Medical, Erlangen, Germany). For this purpose, 185 patients with ALS and 28 healthy controls underwent a protocol consisting of 52 gradients including four *b*₀ gradient directions (*b* = 1000 sec/mm², voxel size ($2.0 \times 2.0 \times 2.8$) mm³, 128×128 pixels, 64 slices, TE = 95 msec, TR = 8000 msec). Sixty patients with ALS and 47 healthy controls underwent a different protocol consisting of 62 gradients including two *b*₀ directions (*b* = 1000 sec/mm², voxel size ($2.5 \times 2.5 \times 2.5$) mm³, 128×128 pixels, 64 slices, TE = 28 msec, TR = 3080 msec). Every MRI scan included a T1-weighted sequence in addition to the DTI sequence.

For post-processing, the DTI analysis software “Tensor Imaging and Fiber Tracking” (TIFT)²² was used. Prior to preprocessing, DTI data underwent quality control for

Table 1. Clinical sample characteristics and cognitive performance of 245 patients with ALS.

	Mean	Standard deviation	Range
Age/years	62.2	11.1	24.6–83.3
Duration since onset/month	21	29	2–251
ALS-FRS-R	39.4	6.0	14–48
Total ECAS score	100.3	20.1	20–128
ECAS fluency	16.9	5.5	0–32
ECAS language	23.7	4.3	6–28
ECAS executive function	34.6	7.9	6–47
ECAS memory	14.6	5.4	0–26
ECAS visuospatial function	11.2	1.8	0–22

ALS, amyotrophic lateral sclerosis; ALS-FRS-R, revised ALS functional rating scale; ECAS, Edinburgh Cognitive and Behavioral ALS Screen.

motion and eddy current correction. DTI datasets were resampled to an isotropic 1 mm grid, followed by nonlinear spatial normalization to the Montreal Neurological Institute (MNI) stereotaxic standard space using study-specific b_0 and FA templates sets iteratively. This normalization procedure was described in more detail previously.²³ Calculated FA maps of each dataset were smoothed with a Gaussian filter of 8 mm full-width-at-maximum. Subgroups of age- and sex-matched controls from both scanning protocols were used for calculation of protocol differences and harmonization.^{24,25}

Fiber tracking

For identification of the relevant tract systems by a tract of interest-based approach, an averaged dataset from control data were used. According to the DTI staging system,^{15,16} the following brain structures were defined with a seed-to-target approach: the corticospinal tract (CST) (stage 1), the corticorubral and corticopontine tracts (stage 2), the corticostriatal pathway (stage 3), and the proximal portion of the perforant pathway (stage 4). Fiber tracking was a deterministic streamline tracking approach.²⁶ The FA threshold was set at 0.2,²⁷ the Eigenvector scalar product threshold was set at 0.9, the seed regions had a radius of 5 mm, and the target regions had a radius of 10 mm. Tract-wise FA statistics was applied to select FA values underlying the fiber tracks for arithmetic averaging. The averaged FA values were tract-wise corrected for age according to a previous study.²⁸ Bihemispheric FA values were averaged, as well as the results of corticopontine and corticorubral tracts since both were involved in DTI stage 2. Tract-wise group comparison with healthy controls were performed using Mann–Whitney U tests.

Eye tracking

Eye movements were recorded using the VOG device EyeSeeCam™ (EyeSeeTec GmbH, Fürstfeldbruck, Germany) in our oculomotor laboratory which is certified in accordance with DIN EN ISO 14971.^{29,30} Participants were seated in a comfortable chair facing a white hemicylindrical screen with their head stabilized by an adjustable chin rest. Visually guided reactive saccades (VGRS) were pseudo-randomly elicited in horizontal (32 target steps between 5° and 40° distance) and in vertical directions (36 target steps between 5° and 30° distance) by lighting red light emission diodes as described previously in more detail.³⁰ Participants were instructed to re-fixate the new target and withhold their gaze shift until the next diode was lit. Rapid alternating voluntary gaze shifts were evoked in horizontal and vertical directions by requesting

participants to perform saccades for 30 sec between two steady green targets with 20° distance.¹⁷ Delayed saccades were tested by presenting a new additive target in 5, 10, 20, and 40° distance when participants were asked to withhold saccades toward the new target until an acoustic “go” cue was given. Anti-saccades were tested by presenting targets at $\pm 5^\circ$, $\pm 10^\circ$, $\pm 15^\circ$, and $\pm 20^\circ$ eccentric horizontal positions. Participants were asked to instantly initiate a gaze shift toward the opposite direction of the new target. Prior to the delayed saccade and anti-saccade condition, a training session was administered.¹⁷

Analysis of eye movements

Analysis of eye movement recordings was carried out with the MATLAB® (The Mathworks Inc., Natick, MA)-based in-house software package “OculoMotor Analysis”.^{17,29,30} The preprocessing pipeline included low-pass filtering, cross-talk suppression, calibration, quality check, and averaging to a cyclopean signal, as described previously in detail.¹⁷ VGRS were characterized by the primary saccade gain and peak eye velocity for horizontal, up, and down. Saccadic intrusion rate was examined during fixation in between VGRS target steps and was computed as the accumulated amplitude of saccades divided by trial time that is, given as “prevalence” in degrees per second. Rapid alternating gaze shifts were counted in both directions and averaged. For delayed and anti-saccade tasks, the percentage of errors was calculated. Parameters were adjusted for age based on the results of the controls.²⁹ Group comparisons of VOG parameters with healthy controls were performed using Mann–Whitney U tests.

Cognitive assessment

Cognitive profile was assessed using the German version of the Edinburgh Cognitive and Behavioral ALS Screen (ECAS)^{31,32} with subdomains of ALS-specific functions (executive function, language, and verbal fluency) and non-ALS-specific functions (memory, visuospatial perception). Age and education adjusted cutoffs were used.³² A lower score was taken to indicate lower cognitive performance. Behavioral changes were assessed by caregiver interviews with regard to disinhibition, apathy, loss of sympathy/empathy,³³ perseverative/stereotyped behavior, hyperorality/altering eating behavior, and psychotic symptoms.

Clustering

The general procedure of data preprocessing and subsequent clustering, implemented using Scikit-learn (version 0.24.2) Python-toolbox,³⁴ is shown in (Fig. 1). First, for

the three domains microstructure, oculomotor function, and cognition, we defined a total of 15 parameters (Table 2) associated with the respective staging criteria.^{3,15,17} Because missing values are a common challenge in clustering, we excluded datasets with missing parameter values. To account for different scales, all indicator parameters were standardized into *z*-scores. Relations between the individual variables were determined as Pearson correlation coefficient with a Bonferroni-corrected significance level. Beyond the domains covered by the cognitive staging approach,³ especially language and verbal fluency are impaired in patients with ALS.^{4,35,36} In order to evaluate whether these two ECAS subdomains can usefully extend the chosen parameter set with regard to multimodal staging and also to test for stability of the multi-parametric analysis, the clustering analysis was additionally performed with this extended parameter set of 17 parameters including ECAS language and ECAS verbal fluency.

To overcome indicator redundancy due to some highly correlated parameters, principal component analysis (PCA) was used to reduce indicator dimension while retaining underlying trends and patterns.³⁷ Briefly, the PCA transforms the parameter into so-called “principal components” (PCs), which are orthogonal and uncorrelated to each other. Each PC is a linear combination of the original parameters and the first PC is aligned with the direction of maximal variance in the parameter space. Thus, PCA is a technique to represent the whole parameter set in a new linear combination of the original parameters, that way per se not reducing the dimensions; in order to select the relevant parameters (and that way to reduce the parameter set for consecutive cluster analysis), Horn’s parallel analysis³⁸ was applied to determine the number of PCs to retain and to use for cluster analysis.

Agglomerative hierarchical clustering¹⁸ with Ward’s linkage criterion was used to detect structures in the

Table 2. Definition of parameters for clustering.

Domain	Abbreviation	Parameter
Diffusion metrics	d1	FA along CST
	d2	FA along corticorubral and corticopontine tracts
	d3	FA along corticostriatal pathway
	d4	FA along proximal portion of perforant path
Oculomotor function	o1	VGRS horizontal latency
	o2	VGRS vertical latency
	o3	VGRS horizontal peak eye velocity
	o4	VGRS up peak eye velocity
	o5	VGRS down peak eye velocity
	o6	Delayed-saccades error rate
	o7	Anti-saccades error rate
	o8	Number of voluntary gaze shifts
	o9	VGRS intrusion rate
Cognition	c1	ECAS memory
	c2	ECAS executive function

The selected parameters are associated with the respective staging approaches of the modalities and characterize diffusion metrics, oculomotor functions, and cognition of patients with amyotrophic lateral sclerosis (ALS). Fractional anisotropy (FA) of the tract systems involved in ALS was studied using a tract-of-interest-based approach. CST, corticospinal tract; ECAS, Edinburgh Cognitive and Behavioral ALS Screen; VGRS, visual guided reactive saccades.

dataset without a priori specifying the number of clusters since the present dataset has no ground truth regarding the neuropathological staging of patients. In this clustering algorithm, each data point, in our case each patient with ALS, starts in its own cluster, which is then iteratively merged pairwise by minimizing the distance until all data points have been merged into one single cluster. A validation via a random division of the sample into a training and validation subsample as commonly used in supervised AI approaches to assess the quality of the algorithm has no advantage for the ex post facto data sample

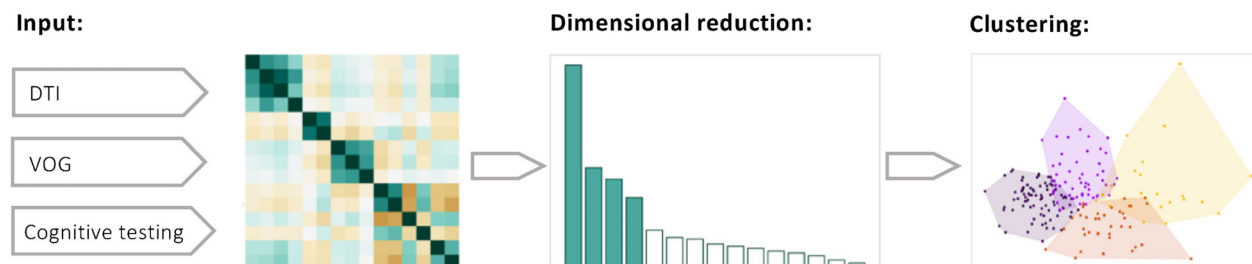


Figure 1. Workflow scheme of multi-parametric cluster analysis in patients with amyotrophic lateral sclerosis (ALS). Input are four microstructural parameters from diffusion tensor imaging (DTI), nine oculomotor parameters obtained by video-oculography (VOG), and two cognitive parameters tested with the Edinburgh Cognitive and Behavioral ALS Screen (ECAS). After standardization, the parameters, some of which were highly correlated, were reduced to four principal components which have the highest explained variance ratio by principal component analysis. Hierarchical and *k*-means clustering are applied to the remaining PCs to find an optimal cluster solution.

of the current study. Since the characteristics of the sample are obligatorily randomly distributed, the results of randomly selected training and validation samples per se would be almost identical and, therefore, the clustering algorithm was performed on the entire sample. Because hierarchical clustering does not present an exact number of clusters as an optimal solution, the number of clusters in the dataset was chosen based on the dendrogram that graphically summarizes cluster partitions and dissimilarities given by the distance between two clusters. To minimize the with-in cluster variances, *k*-means clustering¹⁸ was performed with the centroids of the hierarchical cluster partition as initial centroids. To assess between-cluster

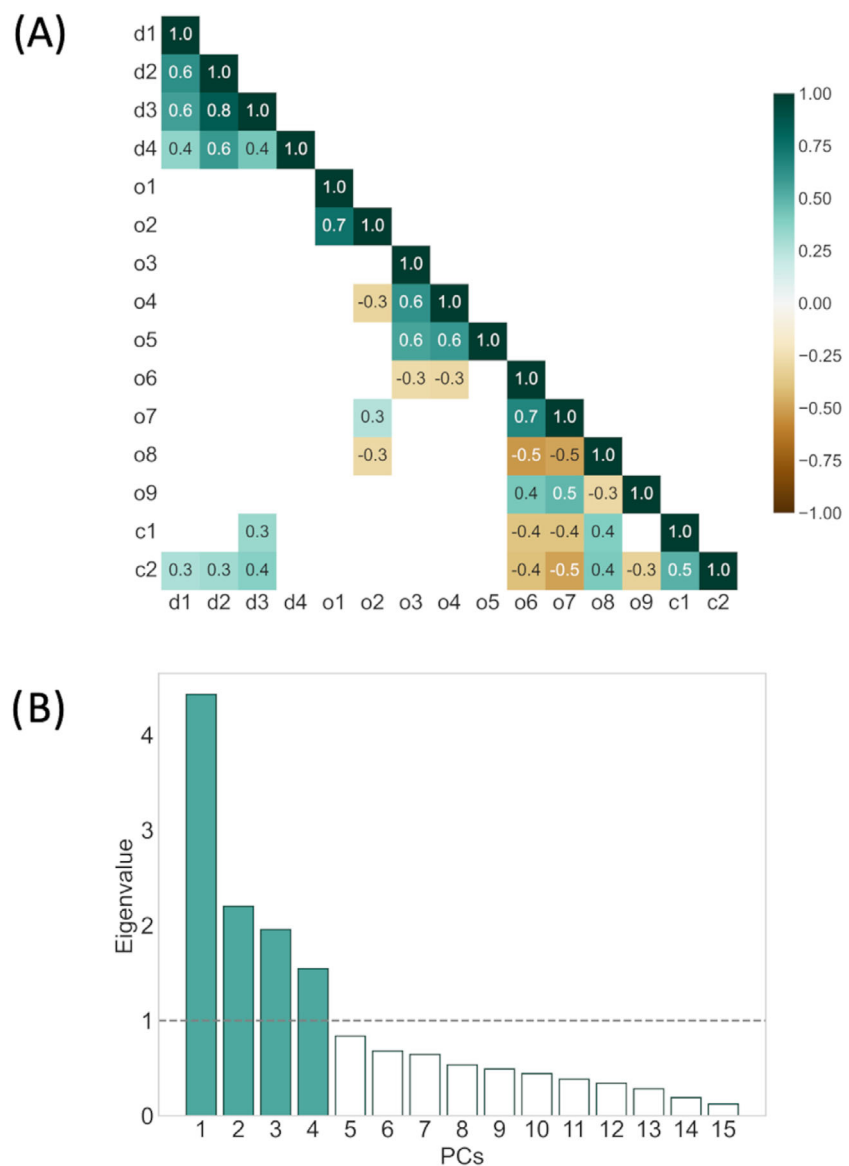
variability, Kruskal–Wallis tests were performed with a Bonferroni-corrected significance level.

Results

Correlation analysis

The correlation coefficients between the selected parameters revealed several strong associations (Fig. 2A). Specifically, the FA values of the studied tract systems were very strongly correlated with each other, and the results of the ECAS executive function part strongly correlated with the results of all executive oculomotor tasks and the ECAS

Figure 2. Correlation between the parameters and results of principal component analysis (PCA). (A) Heatmap of statistically significant Pearson correlation coefficients between different diffusion tensor imaging-based microstructural metrics (d1–d4), oculomotor saccadic metrics (o1–o5), performance in executive oculomotor tasks (o6–o9), and cognitive parameters (c1–c2) of patients with amyotrophic lateral sclerosis (ALS). (B) Eigenvalues for each principal component (PC) after PCA. The first four PCs were retained for cluster analysis.



memory part. In contrast, there were no correlations between any VOG parameter and FA values in the ALS-associated tract systems. Saccadic metrics that is, VGRS latencies and peak eye velocities, showed no or weak correlations with microstructural, executive oculomotor, and cognitive parameters.

Cluster partition

As only participants with complete datasets including all selected VOG parameters were allowed, 53 patients were excluded prior to performing further analyses. According to Horn's analysis after the PCA, the PC set was reduced to the first four PCs with eigenvalues above 1 (Fig. 2B), in sum, explaining 67.21% of the dataset's total variance. PC 1 accounted for 29.38% of the total variance, whereas PC 2, 3, and 4 accounted for 14.60%, 12.97%, and 10.26%. These four PCs were then used for agglomerative hierarchical clustering. The obtained hierarchy of patient cluster arrangements is shown as dendrogram (Fig. 3A). A partition into four clusters provided a good balance between distances and traceability of the number of clusters and their characteristics. After partition refinement using the *k*-means algorithm, cluster A contained 79 patients, cluster B 55 patients, cluster C 37 patients, and

cluster D 21 patients. In (Fig. 3B), the cluster arrangement after *k*-means is shown.

Statistical analysis

Statistical analysis showed that clusters significantly differed in all 15 parameter means with corrected $p < 0.003$. The distribution of all parameters resulting from the partition is shown in (Fig. 4). In general, there was a gradient that is, a decline, in executive VOG performance (anti-saccade and delayed saccades error rate, number of voluntary gaze shifts, VGRS intrusion rate; see (Fig. 4J–M), and cognitive performance (memory and executive function ECAS; Fig. 4N and O) across clusters A to D. A decrease of FA values in all tract systems was also observed simultaneously (Fig. 4A–D). Thus, cluster A was found to have the highest FA scores and simultaneously the best performance in executive VOG tasks and cognitive testing, whereas patients with ALS in cluster D showed the lowest FA scores, the worst executive VOG performance with high anti-saccade and delayed saccades error rates, low numbers of voluntary gaze shifts, high saccadic intrusion rates, and the lowest memory and executive function ECAS scores. A group comparison of VOG parameters between patients belonging to cluster A and

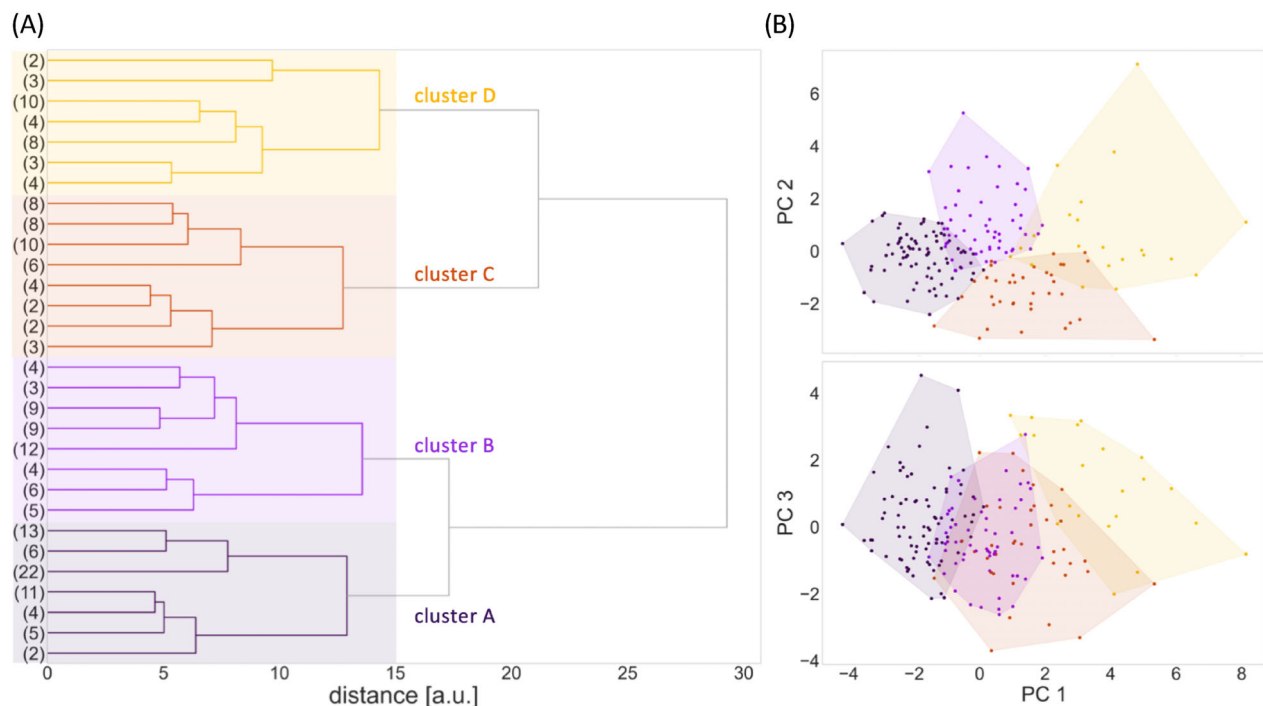


Figure 3. Cluster partition obtained from hierarchical and *k*-means clustering of principal components. (A) The dendrogram of hierarchical clustering was partitioned at a distance threshold of 15. The resulting solution with four clusters is indicated by four colored panels. (B) Scatter plots indicating how clusters were distributed on principal components (PCs) 1–3 after *k*-means clustering (PC 4 was not shown to simplify visualization).

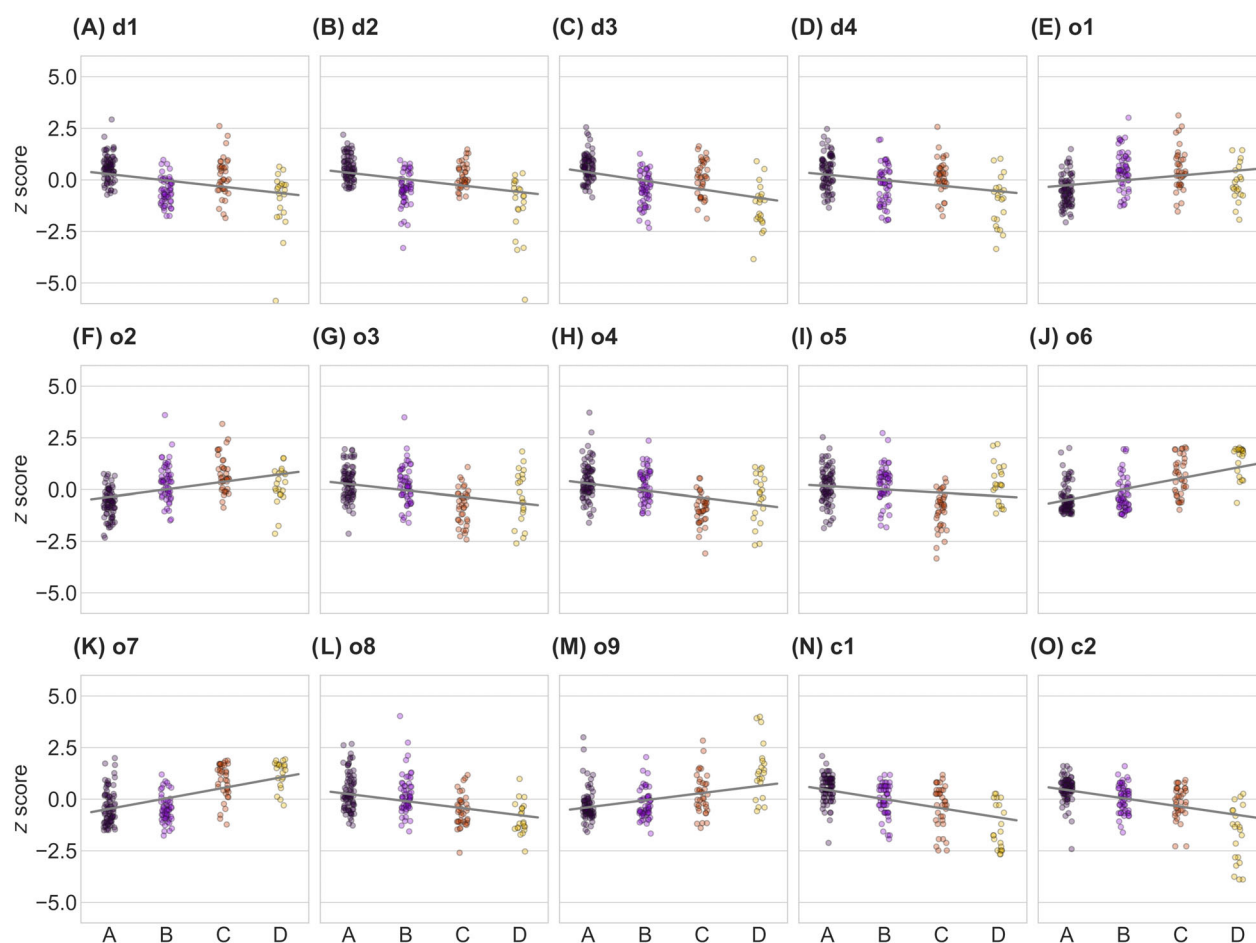


Figure 4. Distribution of parameters within the clusters of patients with ALS. Scatter plots show z-scores of microstructural (A–D), oculomotor (E–M), and cognitive parameters (N and O) for the four clusters A, B, C, and D. Owing to the z-standardization, the values can be interpreted as a deviation from the mean of patients with ALS. Gray line works as a guide to the eye. ALS, amyotrophic lateral sclerosis; CST, corticospinal tract; VGRS, visual guided reactive saccades; ECAS, Edinburgh Cognitive and Behavioral ALS Screen.

healthy controls showed no differences for VGRS latencies, VGRS velocities, VGRS intrusion rate, and number of voluntary gaze shifts. The delayed and anti-saccades error rates were already increased for cluster A ($p < 0.001$ vs. healthy controls), although these were the lowest compared to the other clusters. The obtained metrics of VGRS that is, latencies and peak eye velocities, did not fall into this pattern; cluster C showed the lowest peak eye velocities (Fig. 4G–I), whereas the latencies of cluster A were the shortest.

The comparison of the FA values of cluster D with healthy controls showed statistically significant differences ($p < 0.001$) in all four tract systems, whereas cluster A did not show any significant differences from healthy controls at group level. Cluster B showed lower FA values in the CST, the corticopontine and corticorubral tract systems, and the corticostriatal pathway. Cluster C

showed lower FA values only in the CST. Note in this context that, based on distances and hierarchy (see Fig. 3A), cluster B is more similar to A than it is to C, and cluster C is more similar to D than it is to B.

Extended parameter set

The same clustering procedure including PCA was performed with the extended parameter set that is, including ECAS language and ECAS verbal fluency. With the addition of these two parameters, the PCA resulted in new PCs of the dataset. Now, the selection of PCs used for clustering of this extended parameter set was oriented to the sum of the explained variance of the four PCs used for the 15-parameters-based cluster analysis (i.e., 67.21%). Therefore, the first five PCs were kept, which in sum explained 70.45% of the total variance (Supplementary

Fig. S1); based on those five PCs, agglomerative hierarchical clustering was performed. Again, a partition into four clusters provided a good balance between distances and traceability of the number of clusters and their characteristics (Supplementary Fig. S2). After partition refinement using the *k*-means algorithm, cluster A contained 99 patients, cluster B 13 patients, cluster C 21 patients, and cluster D 55 patients.

The statistical analysis showed that the mean values of the considered parameters differed less than in the clustering based on 15 parameters. Thus, the differences in saccade latencies, VGRS velocities, and the saccadic intrusion rate were not significant. The general trend that is, a decrease or increase in the parameter values across the clusters, was still existent (Supplementary Fig. S3). Thus, cluster A was found to have the highest FA scores and simultaneously the best performance in executive VOG tasks and cognitive testing, whereas patients with ALS in cluster D showed the lowest FA scores, the worst executive VOG performance with high anti-saccade and delayed saccades error rates, low numbers of voluntary gaze shifts, high saccadic intrusion rates, and the lowest memory and executive function ECAS scores.

Discussion

Here, we employed an AI-based approach to investigate the associations between cerebro-microstructural, oculomotor, and cognitive parameters in ALS and, in so doing, incorporated further non-imaging parameters into the *in vivo* disease stage categorization. The correlation between cognitive parameters and microstructural measurements in ALS-associated tract systems could be validated.³ Furthermore, we could demonstrate that the performance of patients with ALS in executive oculomotor tasks, such as anti-saccades or saccadic intrusion rate, correlated strongly with cognitive test scores regarding memory and executive function, which was anticipated owing to frontal involvement in both domains.^{39,40} The additional analysis of further cognitive domains to the staging-related parameters did not improve the results of the clustering analysis that is, the multimodal mapping of neuropathological stages. This constellation supports the selected parameter set (of executive functions and memory) for cognitive staging in ALS.³

AI and machine learning models have been increasingly used in subtype classification in neurological diseases using technical parameters such as imaging⁴¹ and should be explored in ALS for diagnostic, prognosis, and risk stratification applications, inasmuch as they have the potential to surpass traditional approaches.¹⁹ Individualized therapeutic approaches ask for precise patient classification for subgrouping early in the disease course. Thus,

data-driven approaches will extend clinical examination for future clinical trials. Besides promising pilot studies of AI-based diagnostic applications to MRI data of patients with ALS versus healthy controls,⁴² large multivariate datasets might play a role in further improving diagnostic models by incorporating different domains.⁴³ In addition, by including different parameters in subgroup modeling, the impact of bias and confounders in some parameters will be reduced for example, education bias in cognitive function or motor dysfunction in both MRI or oculomotor measurements.

Our multimodal clustering approach was able to show that patients with ALS who performed worst in cognitive tests used to assess memory and executive functions and in tests of executive oculomotor tasks for example, high error rates in delayed and anti-saccade tasks, also showed the lowest FA values across all investigated tracts. In line with this finding, one group of patients (cluster A) was identified, in whom all oculomotor and cognitive parameters were least affected and FA values were the highest. Associations with neuropathological stages could be inferred from group comparisons of patients' FA values with healthy controls. Cluster A with the best executive oculomotor and cognitive performance and the highest FA scores may correspond to neuropathological stage 1. Because significant differences were observed in cluster D in all ALS-associated tract systems, this cluster may represent neuropathological stage 4. It seems safe to assume that in early and late pathological stages, the different modalities show a very high congruence. Aligned between these two clusters, cluster B and C presented with a decreasing congruence of modalities. In cluster C, comparison of microstructural parameters with those of healthy controls showed only a significant difference in FA of the CST, with declined performance in executive oculomotor tasks and cognitive tests compared to cluster B. Based on the alterations in the involved tract systems, there are indications that cluster C may be associated with neuropathological stage 2 and cluster B with neuropathological stage 3. This constellation might indicate that brain dysfunction in distinct areas may be modified by additional factors in different patients with ALS. For instance, asymptomatic *C9orf72* gene carriers exhibit executive oculomotor and cognitive dysfunctions^{29,44} of non-progressive nature which is potentially due to developmental deficits. AI-based diagnostic applications may enable future stratification of disease pathology even in the preclinical phase. During disease progression, there is a close association of clinical subtypes and parameters that could be used for AI-based approaches for example, bulbar involvement is associated with cognition and behavior.^{5,45} Characteristics of saccadic parameters also differ between patients with bulbar or spinal onset, given

that dysmetric saccades are more common in patients with bulbar onset,⁴⁶ whereas upward saccades are delayed in patients with spinal onset.¹⁷ An over-representation of patients with spinal onset in cluster C might be a possible reason why the VGRS down peak eye velocity of this group alone was altered. It has to be noted that, in this approach, only the ALS-associated multisystem pathology according to the proposed propagation pattern¹¹ and not the peripheral pathology (such as the involvement of the second motor neuron) has been addressed because we limited our assessments to central nervous system dysfunction. This constellation might explain why the more altered clusters were not necessarily associated with higher disease burden, which might prominently be linked with the lower motor neuron involvement that was not addressed by the current approach.

This study has further limitations. The results were not confirmed by postmortem examination. Therefore, a combination of multimodal cluster classification and definitive neuropathological stage classification was not possible. Because only cross-sectional data were used, no conclusions can be drawn about whether patients change cluster attribution during disease progression. A final issue could be the selection of the indicators on which the PCA and cluster analysis was based. Behavioral deficits and smooth pursuit eye movement impairment were excluded for methodological reasons, although they play a role in VOG and cognitive staging decisions.^{3,17} Since no multimodal datasets of healthy controls were available, the patients' parameters were compared with different control groups in each modality.

In conclusion, our results support the enormous academic and clinical potential of AI-based approaches in ALS.^{19,47} Cluster analysis of multimodal parameters associated with the respective criteria for staging in DTI, VOG, and cognitive testing displayed a high congruence of these approaches in patients with ALS. The combination of measures of structural changes in diffusion-weighted MRI with measures of cognition and oculomotor function was capable of assessing neuropathological stages 1 and 4 in particular and could provide the basis for a future multimodal extension of the *in vivo* staging system. Such approaches of a deep patient characterization by multiple domains might be further expanded by the use of a greater number of clinical parameters and have the potential to substantially guide patient stratification for clinical trials and for individualized patient care.

Author Contributions

A. B.: study concept and design, data acquisition, data analysis and interpretation, and drafting of manuscript. H.-P. M.: study concept and design, data analysis and

interpretation of data, and critical revision of the manuscript for important intellectual content. K. D. T.: interpretation of data, critical revision of manuscript for important intellectual content. H. B.: interpretation of data, critical revision of manuscript for important intellectual content. A. C. L.: interpretation of data, critical revision of manuscript for important intellectual content. D. L.: data acquisition, interpretation of the data, critical revision of the manuscript for important intellectual content. J. K.: study concept and design, analysis and interpretation, critical revision of manuscript for important intellectual content, and study supervision.

Acknowledgments

The authors would like to thank Mr. Ralph Kühne for help with the eye movement recordings and Ms. Sonja Fuchs for help in the acquisition of MRI data. Further thanks to the Ulm University Center for Translational Imaging MoMAN for its support. Open Access funding enabled and organized by Projekt DEAL. WOA Institution: N/A Consortia Name : Projekt DEAL

Conflict of Interest

The authors report no competing interests.

References

1. Kiernan MC, Vucic S, Cheah BC, et al. Amyotrophic lateral sclerosis. *Lancet*. 2011;377(9769):942-955.
2. Grossman M. Amyotrophic lateral sclerosis—a multisystem neurodegenerative disorder. *Nat Rev Neurol*. 2019;15(1):5-6.
3. Lulé D, Böhm S, Müller HP, et al. Cognitive phenotypes of sequential staging in amyotrophic lateral sclerosis. *Cortex*. 2018;101:163-171.
4. Lulé DE, Aho-Özhan HE, Vázquez C, et al. Story of the ALS-FTD continuum retold: rather two distinct entities. *J Neurol Neurosurg Psychiatry*. 2019;90(5):586-589.
5. Crockford C, Newton J, Lonergan K, et al. ALS-specific cognitive and behavior changes associated with advancing disease stage in ALS. *Neurology*. 2018;91(15):e1370-e1380.
6. Lulé DE, Ludolph AC. In vivo tracking of TDP43 in ALS: cognition as a new biomarker for brain pathology. *J Neurol Neurosurg Psychiatry*. 2020;91(2):125.
7. Schreiber H, Gaigalat T, Wiedemuth-Catrinescu U, et al. Cognitive function in bulbar- and spinal-onset amyotrophic lateral sclerosis. A longitudinal study in 52 patients. *J Neurol*. 2005;252(7):772-781.
8. Bersano E, Sarnelli MF, Solara V, et al. Decline of cognitive and behavioral functions in amyotrophic lateral sclerosis: a longitudinal study. *Amyotroph Lateral Scler Frontotemporal Degener*. 2020;21(5-6):373-379.

9. Donaghy C, Thurtell MJ, Pioro EP, Gibson JM, Leigh RJ. Eye movements in amyotrophic lateral sclerosis and its mimics: a review with illustrative cases. *J Neurol Neurosurg Psychiatry*. 2011;82(1):110-116.
10. Sharma R. Oculomotor dysfunction in amyotrophic lateral sclerosis: a comprehensive review. *Arch Neurol*. 2011;68(7):857.
11. Braak H, Brettschneider J, Ludolph AC, Lee VM, Trojanowski JQ, Tredici KD. Amyotrophic lateral sclerosis—a model of corticofugal axonal spread. *Nat Rev Neurol*. 2013;9(12):708-714.
12. Brettschneider J, Del Tredici K, Toledo JB, et al. Stages of pTDP-43 pathology in amyotrophic lateral sclerosis. *Ann Neurol*. 2013;74(1):20-38.
13. Braak H, Ludolph AC, Neumann M, Ravits J, del Tredici K. Pathological TDP-43 changes in Betz cells differ from those in bulbar and spinal α -motoneurons in sporadic amyotrophic lateral sclerosis. *Acta Neuropathol*. 2017;133(1):79-90.
14. Ludolph AC, Brettschneider J. TDP-43 in amyotrophic lateral sclerosis - is it a prion disease? *Eur J Neurol*. 2015;22(5):753-761.
15. Kassubek J, Müller HP, Del Tredici K, et al. Diffusion tensor imaging analysis of sequential spreading of disease in amyotrophic lateral sclerosis confirms patterns of TDP-43 pathology. *Brain*. 2014;137(6):1733-1740.
16. Kassubek J, Müller HP, Del Tredici K, et al. Imaging the pathoanatomy of amyotrophic lateral sclerosis in vivo: targeting a propagation-based biological marker. *J Neurol Neurosurg Psychiatry*. 2018;89(4):374-381.
17. Gorges M, Müller HP, Lulé D, et al. Eye movement deficits are consistent with a staging model of pTDP-43 pathology in amyotrophic lateral sclerosis. *PLoS One*. 2015;10(11):e0142546.
18. Jain AK. Data clustering: 50 years beyond K-means. *Pattern Recognit Lett*. 2010;31(8):651-666.
19. Grollemund V, Pradat P-F, Querin G, et al. Machine learning in amyotrophic lateral sclerosis: achievements, pitfalls, and future directions. *Front Neurosci*. 2019;13:135.
20. Brooks BR, Miller RG, Swash M, Munsat TL. El Escorial revisited: revised criteria for the diagnosis of amyotrophic lateral sclerosis. *Amyotroph Lateral Scler Other Motor Neuron Disord*. 2000;1(5):293-299.
21. Cedarbaum JM, Stambler N, Malta E, et al. The ALSFRS-R: a revised ALS functional rating scale that incorporates assessments of respiratory function. *J Neurol Sci*. 1999;169(1-2):13-21.
22. Müller HP, Unrath A, Ludolph AC, Kassubek J. Preservation of diffusion tensor properties during spatial normalization by use of tensor imaging and fibre tracking on a normal brain database. *Phys Med Biol*. 2007;52(6):N99-N109.
23. Müller HP, Unrath A, Huppertz H-J, Ludolph AC, Kassubek J. Neuroanatomical patterns of cerebral white matter involvement in different motor neuron diseases as studied by diffusion tensor imaging analysis. *Amyotroph Lateral Scler*. 2012;13(3):254-264.
24. Roskopf J, Müller HP, Dreyhaupt J, Gorges M, Ludolph AC, Kassubek J. Ex post facto assessment of diffusion tensor imaging metrics from different MRI protocols: preparing for multicentre studies in ALS. *Amyotroph Lateral Scler Frontotemporal Degener*. 2015;16(1-2):92-101.
25. Kalra S, Müller HP, Ishaque A, et al. A prospective harmonized multicenter DTI study of cerebral white matter degeneration in ALS. *Neurology*. 2020;95(8):e943-e952.
26. Müller HP, Unrath A, Riecker A, Pinkhardt EH, Ludolph AC, Kassubek J. Intersubject variability in the analysis of diffusion tensor images at the group level: fractional anisotropy mapping and fiber tracking techniques. *Magn Reson Imaging*. 2009;27(3):324-334.
27. Kunitatsu A, Aoki S, Masutani Y, et al. The optimal trackability threshold of fractional anisotropy for diffusion tensor tractography of the corticospinal tract. *Magn Reson Med Sci*. 2004;3(1):11-17.
28. Behler A, Kassubek J, Müller HP. Age-related alterations in DTI metrics in the human brain—consequences for age correction. *Front Aging Neurosci*. 2021;13:682109.
29. Behler A, Knehr A, Finsel J, et al. Eye movement alterations in presymptomatic C9orf72 expansion gene carriers. *J Neurol*. 2021;268:3390-3399.
30. Wunderlich J, Behler A, Dreyhaupt J, Ludolph AC, Pinkhardt EH, Kassubek J. Diagnostic value of video-oculography in progressive supranuclear palsy: a controlled study in 100 patients. *J Neurol*. 2021;268:3467-3475.
31. Lulé D, Burkhardt C, Abdulla S, et al. The Edinburgh Cognitive and Behavioural Amyotrophic Lateral Sclerosis Screen: a cross-sectional comparison of established screening tools in a German-Swiss population. *Amyotroph Lateral Scler Frontotemporal Degener*. 2015;16(1-2):16-23.
32. Loose M, Burkhardt C, Aho-Özhan H, et al. Age and education-matched cut-off scores for the revised German/Swiss-German version of ECAS. *Amyotroph Lateral Scler Frontotemporal Degener*. 2016;17(5-6):374-376.
33. Lulé D, Michels S, Finsel J, et al. Clinicoanatomical substrates of selfish behaviour in amyotrophic lateral sclerosis – an observational cohort study. *Cortex*. 2022;146:261-270.
34. Pedregosa F, Varoquaux G, Gramfort A, et al. Scikit-learn: machine learning in python. *arXiv:1201.0490 [cs]*. 2018. Accessed September 22, 2021. <http://arxiv.org/abs/1201.0490>
35. Taylor LJ, Brown RG, Tsermentseli S, et al. Is language impairment more common than executive dysfunction in amyotrophic lateral sclerosis? *J Neurol Neurosurg Psychiatry*. 2013;84:494-498.

36. Niven E, Newton J, Foley J, et al. Validation of the Edinburgh Cognitive and Behavioural Amyotrophic Lateral Sclerosis Screen (ECAS): a cognitive tool for motor disorders. *Amyotroph Lateral Scler Frontotemporal Degener.* 2015;16(3–4):172–179.
37. Lever J, Krzywinski M, Altman N. Principal component analysis. *Nat Methods.* 2017;14(7):641–642.
38. Horn JL. A rationale and test for the number of factors in factor analysis. *Psychometrika.* 1965;30(2):179–185.
39. Becker W, Gorges M, Lulé D, Pinkhardt E, Ludolph AC, Kassubek J. Saccadic intrusions in amyotrophic lateral sclerosis (ALS). *J Eye Mov Res.* 2019;12(6):8.
40. Proudfoot M, Menke RAL, Sharma R, et al. Eye-tracking in amyotrophic lateral sclerosis: a longitudinal study of saccadic and cognitive tasks. *Amyotroph Lateral Scler Frontotemporal Degener.* 2015;17(1–2):101–111.
41. Eshaghi A, Young AL, Wijeratne PA, et al. Identifying multiple sclerosis subtypes using unsupervised machine learning and MRI data. *Nat Commun.* 2021; 12(1):2078.
42. Bede P, Iyer PM, Finegan E, Omer T, Hardiman O. Virtual brain biopsies in amyotrophic lateral sclerosis: diagnostic classification based on in vivo pathological patterns. *Neuroimage Clin.* 2017;15:653–658.
43. Zandonà A, Vasta R, Chiò A, Di Camillo B. A dynamic Bayesian network model for the simulation of amyotrophic lateral sclerosis progression. *BMC Bioinformatics.* 2019;20(S4):118.
44. Lulé DE, Müller HP, Finsel J, et al. Deficits in verbal fluency in presymptomatic *C9orf72* mutation gene carriers —a developmental disorder. *J Neurol Neurosurg Psychiatry.* 2020;91(11):1195–1200.
45. Abrahams S, Goldstein LH, Al-Chalabi A, et al. Relation between cognitive dysfunction and pseudobulbar palsy in amyotrophic lateral sclerosis. *J Neurol Neurosurg Psychiatry.* 1997;62(5):464–472.
46. Kang B-H, Kim J-I, Lim Y-M, Kim K-K. Abnormal oculomotor functions in amyotrophic lateral sclerosis. *J Clin Neurol.* 2018;14(4):464–471.
47. Bede P, Murad A, Hardiman O. Pathological neural networks and artificial neural networks in ALS: diagnostic classification based on pathognomonic neuroimaging features. *J Neurol.* 2021. doi:10.1007/s00415-021-10801-5

Supporting Information

Additional supporting information may be found online in the Supporting Information section at the end of the article.

Figure S1 Explained variance ratio of principal components (PCs).

Figure S2 Cluster partition obtained from hierarchical clustering.

Figure S3 Distribution of parameters within the clusters of patients with amyotrophic lateral sclerosis (ALS).